Geoengineering potential of artificially enhanced silicate weathering of olivine

Peter Köhler[a,1], Jens Hartmann[b], and Dieter A. Wolf-Gladrow[a]

[a]Alfred Wegener Institute for Polar and Marine Research (AWI), P.O. Box 12 01 61, D-27515 Bremerhaven, Germany; and [b]Institute for Biogeochemistry and Marine Chemistry, KlimaCampus, Universität Hamburg, Bundesstrasse 55, 20146 Hamburg, Germany

Edited by Hans-Joachim Schellnhuber, Potsdam Institute for Climate Impact Research, Potsdam, Germany, and approved October 4, 2010 (received for review January 14, 2010)

Geoengineering is a proposed action to manipulate Earth's climate in order to counteract global warming from anthropogenic greenhouse gas emissions. We investigate the potential of a specific geoengineering technique, carbon sequestration by artificially enhanced silicate weathering via the dissolution of olivine. This approach would not only operate against rising temperatures but would also oppose ocean acidification, because it influences the global climate via the carbon cycle. If important details of the marine chemistry are taken into consideration, a new mass ratio of CO_2 sequestration per olivine dissolution of about 1 is achieved, 20% smaller than previously assumed. We calculate that this approach has the potential to sequestrate up to 1 Pg of C per year directly, if olivine is distributed as fine powder over land areas of the humid tropics, but this rate is limited by the saturation concentration of silicic acid. In our calculations for the Amazon and Congo river catchments, a maximum annual dissolution of 1.8 and 0.4 Pg of olivine seems possible, corresponding to the sequestration of 0.5 and 0.1 Pg of C per year, but these upper limit sequestration rates come at the environmental cost of *p*H values in the rivers rising to 8.2. Open water dissolution of fine-grained olivine and an enhancement of the biological pump by the rising riverine input of silicic acid might increase our estimate of the carbon sequestration, but additional research is needed here. We finally calculate with a carbon cycle model the consequences of sequestration rates of 1–5 Pg of C per year for the 21st century by this technique.

alkalinity enhancement | river alkalization | diatoms | biological production | climate engineering

Anthropogenic carbon emissions lead not only to the rise of near surface global temperatures, but also to ocean acidification (1). Besides the need of society to reduce future anthropogenic emissions as addressed in the United Nations Framework Convention on Climate Change to avoid dangerous climate change (2–6), CO_2 sequestration and various geoengineering concepts were proposed to counteract global warming (7, 8). These concepts focus either on the restriction of the proposed temperature rise through an artificial enhancement of the planetary albedo (9, 10) [solar radiation management (SRM)] or on removing CO_2 from the atmosphere by various carbon dioxide removal (CDR) techniques (11–14). The SRM techniques leave the carbon cycle untouched and thus do not address the problem of ocean acidification. The unabated increase of atmospheric CO_2 that accompanies SRM techniques would for some of the Intergovernmental Panel on Climate Change (IPCC) emission scenarios (15) lead to a drop in *p*H of the surface water of up to 0.4 and to a drop in the aragonite saturation state by a factor of 2 in the year 2100 (16). It would thus bring various marine calcifying species, which depend in the buildup of their hard shells or skeletons on the oversaturation of $CaCO_3$ in surface waters, into unfavorable environmental conditions, to which their degree of adaption is yet unknown (1). In the worst case their carbonate parts might dissolve (17).

We investigate in more detail a specific CDR technique, carbon sequestration by artificially enhanced silicate weathering via the dissolution of olivine (18) as a geoengineering technique mitigating both global warming and ocean acidification. Our results expand previous studies on the impact of natural weathering in the future (19–21). Olivine (Mg_2SiO_4) is a well-studied mineral with known dissolution kinetics (22) and has been suggested to be useful for CDR geoengineering (18). Please note that there are a few alternative CDR approaches, which operate via the dissolution of $CaCO_3$ (23–25). According to Schuiling and Krijgsman (18), olivine dissolves in water after

$$Mg_2SiO_4 + 4CO_2 + 4H_2O \Rightarrow 2Mg^{2+} + 4HCO_3^- + H_4SiO_4. \quad [1]$$

This formula suggests that 4 mol of CO_2 are sequestered by 1 mol of olivine, equivalent to 1.25 t of CO_2 (or 0.34 t of C) per tonne of olivine. However, because of the chemistry of CO_2 in seawater (26), the impact of olivine dissolution on the carbon cycle is more complicated because both dissolved inorganic carbon (DIC) and total alkalinity (TA) are changed, leading to a new CO_2 concentration. Thus, the ratio of CO_2 sequestration to olivine dissolution will vary with the initial state of the marine carbonate system and the amount of olivine dissolved. The value of 1.25 t of CO_2 per tonne of olivine is an upper theoretical limit.

The dissolution of olivine leads to an increase of TA by 4 mol per 1 mol of olivine dissolved ([**1**]). If the olivine dissolution reduces atmospheric CO_2 by x μatm (or $x \cdot 2.12$ Pg of C) and if this C is transferred as riverine input of bicarbonate (HCO_3^-) to the surface ocean, the DIC in the surface ocean thus changes from DIC_i to

$$DIC(x) = DIC_i + \frac{2.12 \cdot 10^{15}}{12 \cdot 10^{-3}} \cdot \frac{x}{V_s}, \quad [2]$$

where DIC is in mmol m^{-3} and V_s is the considered ocean surface volume (e.g., the upper 100 m of the ocean are about 3×10^{16} m^3). The factor 12 refers to the molar weight of C (12 g mol^{-1}). From $DIC(x)$ and $pCO_2(x) = pCO_{2i} - x$, one can calculate $TA(x)$ (26) [*SI Text*], and finally, the amount of olivine requested, y (in grams), for a planned sequestration is calculated from TA (mmol m^{-3}) by

$$y(x) = \frac{140}{4} \cdot 10^{-3}[TA(x) - TA_i] \cdot V_s. \quad [3]$$

Author contributions: P.K., J.H., and D.A.W.-G. designed research; P.K. performed carbon cycle simulations; D.A.W.-G. performed calculations of the marine carbonate system; and P.K., J.H., and D.A.W.-G. wrote the paper.

The authors declare no conflict of interest.

This article is a PNAS Direct Submission.

Freely available online through the PNAS open access option.

[1]To whom correspondence should be addressed. E-mail: Peter.Koehler@awi.de.

This article contains supporting information online at www.pnas.org/lookup/suppl/doi:10.1073/pnas.1000545107/-/DCSupplemental.

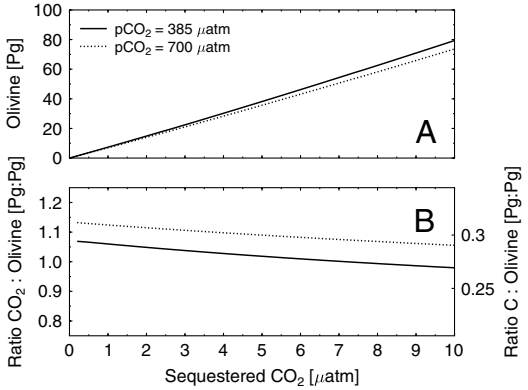

Fig. 1. The dependency of olivine dissolution on initial conditions ($pCO_2 = 385$ or 750 ppmv). (*A*) The amount of olivine necessary for CO_2 sequestration. (*B*) The sequestration ratio (amount of CO_2 sequestered per amount of olivine dissolved).

We plot the resulting relationship between the desired amount of CO_2 to be sequestrated and the amount of olivine necessary to be dissolved in Fig. 1*A*.

The ratio of CO_2 sequestration to the amount of olivine requested is on the order of 1 $g\,g^{-1}$ (ratio C:olivine between 0.25 and 0.3 $g\,g^{-1}$) (Fig. 1*B*). Thus, considering these details on the marine chemistry alone reduces the efficiency of the approach by about 20%. However, in these calculations we assumed that the surface ocean is well mixed. If olivine enters the ocean via rivers, the oceanic volume initially involved in sequestration would be much smaller. Accordingly, the changes in TA and *p*H in this smaller volume would be much larger and thus might have major impacts on aquatic (riverine and coastal) ecosystems.

Results and Discussion

Chemical Consequences for the River Catchments. We provide an upper estimate of CO_2 sequestration with the help of olivine on land, if the *p*H of major rivers in the humid tropics, such as the Amazon or Congo, should not rise above a certain threshold. We use information of riverine partial pressure of CO_2, alkalinity, and runoff of both rivers (Table 1) and calculate for freshwater (27) and a temperature of 25 °C the potential to transport dissolved olivine to the ocean if the maximum tolerable annual average *p*H threshold of 8.0 or 9.0 should not be reached. After Eq. **3**, the annual input of 1.37 and 15.81 Pg of dissolved olivine in the Amazon or of 0.21 and 2.33 Pg of olivine in the Congo catchment area would then be possible. This sequestration rate requires the distribution of 57–2,712 $g\,m^{-2}\,y^{-1}$ of olivine powder throughout the whole area. The enhanced silicate weathering flux would according to Fig. 1 sequestrate approximately as many grams of CO_2 (or 27.5% as much in grams of C) as olivine was dissolved. This procedure would give the Amazon and Congo river basins the artificial silicate weathering potentials to sequester annually up to 4.35 and 0.64 Pg of carbon, respectively.

However, these estimates so far do not address the difficulties in distributing olivine powder in remote land areas covered with dense tropical rain forests and neglect a crucial limitation of the chemistry of olivine dissolution, which is the saturation of waters with silicic acid (H_4SiO_4), which would restrict further dissolution of olivine. The saturation concentration of H_4SiO_4 at 25 °C and *p*H of 8 is ~2,000 $mmol\,m^{-3}$ (28), about a factor of 400 higher than the recent concentration of dissolved Si of 5 $mmol\,m^{-3}$ in the surface ocean (29). If taken at face value, silicic acid saturation would apply a much stronger constraint on the possible olivine dissolution than our *p*H threshold of 9, allowing only an annual input of 1.77 and 0.37 Pg of olivine into the Amazon and Congo, respectively, leading to a *p*H of 8.2 and restricting C sequestration in these catchments to 0.49 and 0.10 Pg of C per y^{-1}. For a more detailed analysis, the rise in solubility of silicic acid with *p*H above 8 needs to be taken into consideration (28).

The river runoff of the Amazon and Congo contributes to more than 50% of the runoff of the 39 largest river basins globally (30). Consequently, the olivine sequestration technique has only limited potential to reduce atmospheric CO_2 in orders of magnitude being of interest in geoengineering (a maximum C sequestration of 1 Pg of C per year), if applied over major catchment areas, either in the tropics or elsewhere. The tropical areas are of special interest because of the *p*H and temperature dependency of olivine dissolution (22). The calculations above are rough estimates, because of the strong seasonality of pCO_2 in tropical rivers (31) and the large spatial gradient downstream. Organic matter degradation leads to supersaturation of rivers and lakes with respect to the atmospheric CO_2 concentrations (32, 33). In the Amazon the CO_2 supersaturation is reduced to zero and reversed to an undersaturation in the river plume that is caused by CO_2 outgassing and a plankton bloom, the latter generated by the riverine input of nutrients (34). The natural fluctuations in riverine pCO_2 lead already to fluctuations in *p*H between 6.4 and 7.8 in the Amazon and 5.7 and 7.6 in the Congo, which also varies the potential allowable anthropogenic input of alkalinity to stay below given *p*H thresholds (Table 1).

Table 1. Chemical consequences of olivine input into the Amazon and Congo river catchment areas (30–32, 54)

	Units	Amazon			Congo		
Catchment area	10^{12} m^2		5.83			3.60	
Runoff	10^{12} $m^3\,y^{-1}$		6.3			1.3	
TA	$mmol\,m^{-3}$		460			250	
pCO_2*	μatm		4,350 (385–13,000)			3,200† (385–35,600)	
*p*H‡	-		6.84 (6.38–7.89)			6.71 (5.67–7.63)	
Resulting *p*H	-	8.0	8.2§	9.0	8.0	8.2§	9.0
Δ(TA)¶	$mmol\,m^{-3}$	6,192	8,040	71,631	4,646	8,040	52,786
Flux (TA)	10^{12} $mol\,y^{-1}$	39	51	452	5.9	10.5	66.6
Flux (olivine)‖	$Pg\,y^{-1}$	1.37	1.77	15.81	0.21	0.37	2.33
ρ(olivine)	$g\,m^{-2}\,y^{-1}$	234	305	2712	57	100	647
C sequestration**	Pg of C per year	0.38	0.49	4.35	0.06	0.10	0.64

*Mean riverine pCO_2 is framed by a minimum pCO_2 identical to the present-day atmospheric value (385 μatm) and a maximum value given by observations.
†pCO_2 for the Congo river was not available; thus, we took the global mean from 47 larger rivers (32) framed by the maximum value given by an African river (Niger) in the compilation.
‡The corresponding *p*H was calculated on the total *p*H scale from pCO_2 for fixed given TA (26), neglecting the effect of organic matter respiration (the main process responsible for the supersaturation of CO_2 with respect to the atmosphere in the rivers) on TA.
§Olivine dissolution leads to H_4SiO_4 saturation concentration of 2,000 $mmol\,m^{-3}$ in the river.
¶ΔTA calculated for freshwater conditions (27).
‖The flux of olivine is following Eq. **3**.
**Assuming a CO_2:olivine ratio of 1 $g\,g^{-1}$.

In addition, the dissolution rate of olivine depends on the reactive surface and thus decreases with grain size. Small grain sizes (10 μm) are necessary to allow fast dissolution of olivine within 1 or 2 y considering the typical *p*H conditions of tropical soils (*p*H 4–6) (22) and the high application rates that are required to obtain a significant CO_2 sequestration. Our ratio of CO_2 sequestration to olivine dissolution is therefore an upper limit for favorable conditions and under the assumption of a complete dissolution. The net CO_2 sequestration efficiency will be reduced by 5–10% because of CO_2 emissions by mining and grinding of olivine (22). The less energy-demanding grinding to a 37-μm size would cause only a decrease of the net efficiency by 0.7–1.5% because of differences in grinding techniques (22) but may not be sufficient for the attempted fast dissolution rates. In addition, transport decreases the net efficiency by 2.4%, 1.6%, and 11% per 1,000 km of transport for inland and coastal ships, freight trains, and trucks, respectively (22, 35). Fortunately, suitable dunite complexes for mining of olivine are located in the humid tropical regions, to allow relatively short ways for the transport of olivine powder to application sites (Fig. 2). Thus, the CO_2 net efficiency of olivine dissolution for applications within 1,000 km of mines can be 93%. Costs for mining and grinding are estimated (22) to be €10 per tonne of sequestered CO_2 (€37 per tonne of C). Taking into account costs for applications (36), total costs might be in the range of €20–40 per tonne of CO_2 sequestered (or €70–150 per tonne of C). These costs may be compensated by CO_2-emission–certificate trade (37).

Considering a sequestration of 0.5 Pg of C per year requires an olivine distribution rate of about 300 $g\,m^{-2}\,y^{-1}$, if applied over the whole Amazon catchment area (Table 1). This procedure would lead to enhanced weathering rates of 85 t of C per $km^{-2}\,y^{-1}$, respectively, which is at the upper range of reported natural basalt weathering rates in humid tropical regions (38). Thus, from field and laboratory evidence as well as from models (22, 38), it is reasonable to assume that the geoengineering potential of enhanced silicate weathering by the dissolution of olivine in the humid tropics is on the order of 1 Pg of C per year. This estimate considers the limitation by the saturation of silicic acid and assumes a complete dissolution of all distributed olivine. Furthermore, it is necessary that applicable areas are identified and the demanded infrastructure is being built up. It seems, however, unrealistic that the required distribution rates might be applied over remote regions of these catchment areas because of practical reasons.

The C sequestration rates might be increased above this potential by two additional effects.

First, olivine powder might also be dissolved in open ocean surface waters. It is known that 50–60% of biogenic-produced silica (opal) is redissolved in the upper 100 m of the water column (39); thus, anthropogenic-distributed fine grain olivine powder also has the potential to be partially dissolved in the surface of the open ocean. As the net effect of olivine dissolution, TA increases by 4 mol per 1 mol of olivine dissolved whereas DIC stays constant ([**1**]). This change in TA reduces the partial pressure of CO_2 in the surface ocean, leading to an additional oceanic uptake of CO_2 from the atmosphere via gas exchange (26). This way of dissolving olivine is, however, much less efficient than on land, because of the higher oceanic *p*H reducing the dissolution rate (22) and the considerable large fraction that will sink undissolved to the ocean floor.

Second, the rise in riverine input of silicic acid into the world oceans accompanying olivine dissolution on land might enhance the marine biological pump. Silicate is known to be a limiting factor for diatoms in various parts of the world ocean (40). With diatoms being responsible for about 50% of marine export production (41), an enhanced riverine input of dissolved silicate (42) has the potential to largely alter the biological pump, although the overall net effect is, because of the high dissolution rates in the euphotic zone (39), difficult to estimate.

Both effects need future investigations to finally quantify their contribution to the C sequestration potential introduced by olivine dissolution.

Global Carbon Cycle Dynamics. To set these sequestration rates into context with the assumed evolution of fossil fuel emissions and climate change in this century, we implemented them in a carbon cycle box model. We compare nonweathering control runs with artificial enhanced weathering for A2 and B1 IPCC emission scenarios (see *Materials and Methods*). We imply C sequestration rates of 1 or 5 Pg of C per year. The first is the potential of olivine dissolution on tropical land, and the latter is an upper limit in a scenario with additional dissolution in tropical open ocean surface waters or on suitable areas outside the tropical regions. It might, for example, be obtained if annually 40 g of C per m^{-2} are sequestrated by the dissolution of 150 g of olivine per m^2 over the entire tropical ocean waters ($\sim 100 \cdot 10^{12}$ m^2). Olivine distribution rates for that scenario are difficult to estimate, because of the second-order effect of marine productivity and carbonate chemistry as mentioned above, and warrant additional research. In the control runs without artificial silicate weathering (Fig. 3), atmospheric pCO_2 in the A2 emission scenario rises to 720–960 μatm in A.D. 2100 depending on the dynamics of the terrestrial C storage. This range in atmospheric pCO_2 covers

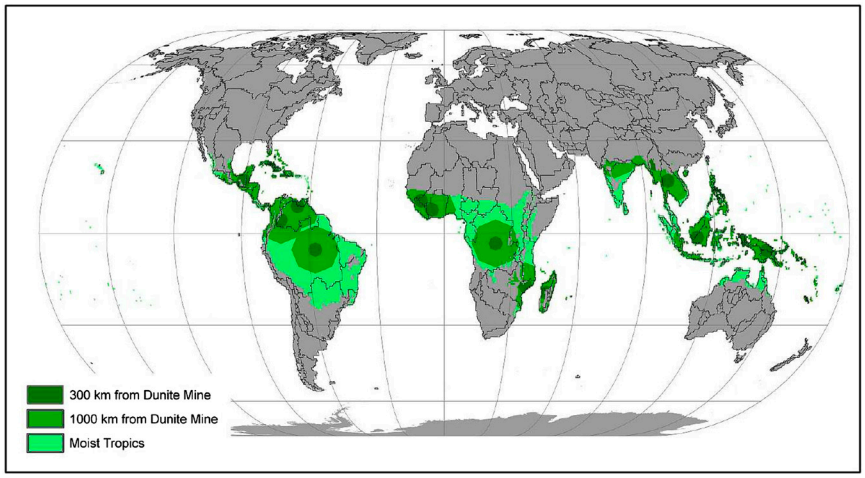

Fig. 2. Location of some active dunite mines in the humid tropics plotted together with coastal segment (53). There exist, however, more locations that could be mined for dunite.

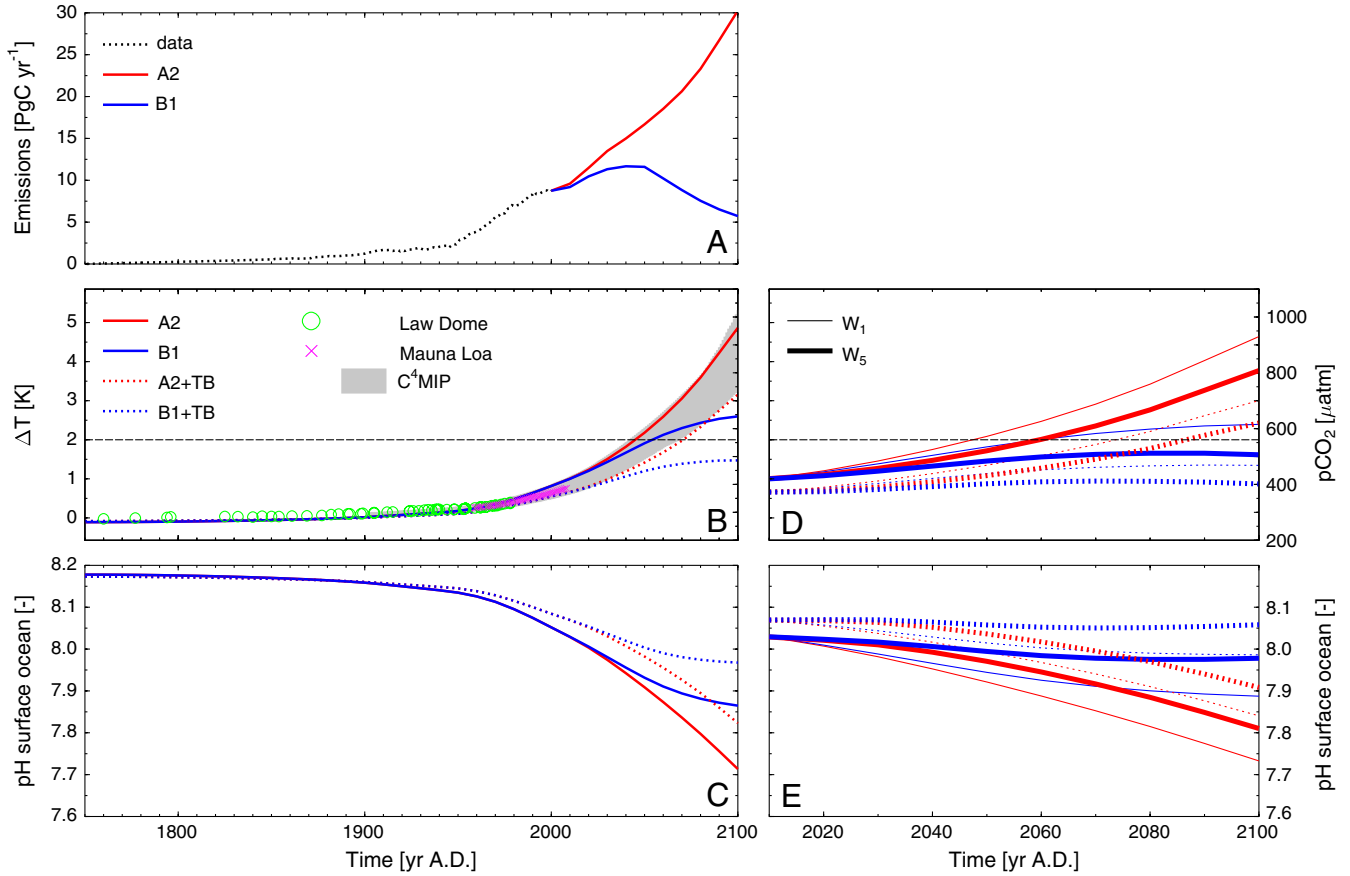

Fig. 3. Simulating the consequences of olivine dissolution for the global carbon cycle. (*A*) The sum of anthropogenic emissions from fossil fuel combustion (A.D. 1750–2000) (51) and land use change (A.D. 1850–2000; before A.D. 1850: linear extrapolation of land use change to zero in A.D. 1750) (50). A.D. 2000–2100: Projected emission for A2 and B1 scenarios (15). (*B*) Global transient temperature rise (left *y* axis) inter(extra)polated from a transient climate sensitivity of 2 K for a doubling of preindustrial atmospheric CO_2 (52) and atmospheric CO_2 (right *y* axis), data from Law Dome ice core (45), and instrumental measurements on Mount Mauna Loa A.D. 1958–2008 (46). Simulation results of the emission scenarios without (A2 and B1) and with (A2 + TB and B1 + TB) dynamical terrestrial carbon storage. The gray area covers the range of results from coupled carbon cycle-climate simulations for the A2 emission scenario C^4MIP (43). (*D*) Impact of enhanced silicate weathering for A.D. 2010–2100. Global temperature rise (left *y* axis) and simulated atmospheric pCO_2 (right *y* axis) for the A2 and B1 scenarios with and without dynamical terrestrial carbon storage for three different weathering strengths [W_1 (thin line):+1 Pg of C per year; W_5 (bold line): +5 Pg of C per year]. (*C* and *E*): Mean *p*H of the global surface ocean for the same scenarios as in *B* and *D*, respectively. Dotted horizontal lines in *B* and *D* denote the 2-K warming threshold.

the spread of the coupled carbon cycle-climate simulations of C^4MIP (43), although it should be noted that C^4MIP neglects feedbacks from the nitrogen cycle, which is nowadays known to have a significant impact on C storage on land (44). The agreement between A.D. 1750 and A.D. 2000 of the simulations with both Law Dome ice core reconstructions (45) and instrumental measurements on Mauna Loa (46) is reasonable. Simulated pCO_2 in the more optimistic emission scenario B1 reaches values of 490–640 μatm. The rise in pCO_2 would approximately lead to a global warming in A.D. 2100 of 1.5–4.9 K. They are furthermore accompanied by a drop in mean surface ocean *p*H of 0.36–0.41 (A2) and 0.20–0.31 (B1) in A.D. 2100 if compared with preindustrial times.

The simulated transient behavior of atmospheric pCO_2 and mean surface ocean *p*H for all scenarios with artificial silicate weathering are compiled in Fig. 3 *D* and *E*. In the most optimistic case (B1 emission scenario and maximum artificial weathering W_5) pCO_2 stabilizes around 400–600 μatm, and *p*H drops only to ~8.0. If a maximum global mean warming of 2 K until A.D. 2100 is the main target (4), then emissions have to follow B1, and at least the CO_2 sequestration of the weak weathering scenario W_1 is necessary. If emissions follow the A2 scenario, the geoengineering concept of olivine dissolution is not capable of reaching the 2-K warming target (Fig. 3*D*).

The weak artificial weathering rate, which sequesters 1 Pg of C per year, reduces pCO_2 by less than 30 μatm (equivalent to a global warming that is 0.2 K smaller than in the control runs) in the year 2100 and increases *p*H by about 0.02, regardless of the emission scenario and our assumption on the dynamics of the terrestrial C storage (Fig. 4). The strong enhanced weathering (5 Pg of C per year) would reduce pCO_2 by 80–150 μatm (global warming reduced by 0.6–1.1 K) and increases *p*H by about 0.1 in year 2100. In all these simulations the emission scenarios are less important for the calculated impact on the C cycle than the assumptions on the terrestrial C storage.

Altogether, enhanced weathering via the dissolution of fine-grained olivine powder on land in the humid tropics seems to be a CDR technique, which might sequester up to 1 Pg of C per year directly. This technique has certain geoengineering potential, although the applicable ratio of CO_2 sequestration per olivine dissolution is 20% smaller than previously assumed. The efficiency of olivine dissolution in the open ocean needs further investigation, and the second-order effect of an enhanced biological pump due to increased riverine input of silicic acid needs to be evaluated with both models and field studies. The technique is not able to compensate alone for rising emissions under business-as-usual scenarios. Once emissions are reduced from present-day values to about half (~4 Pg of C per year), it

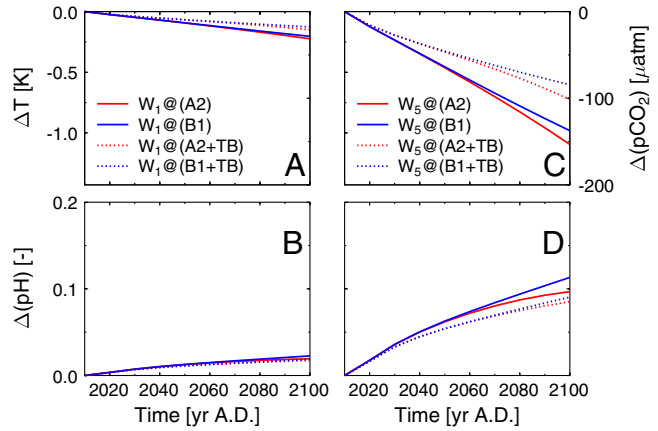

Fig. 4. Differences in global temperature, atmospheric pCO_2, and mean surface ocean *p*H induced by enhanced silicate weathering for A.D. 2010–2100. (*A* and *B*) Weak weathering scenario W_1: +1 Pg of C per year. (*C* and *D*) Strong weathering scenario W_5: +5 Pg of C per year. Both *y* axes in *A* and *C* are for both subfigures.

might help to quickly extract a large part of the residual fossil fuel inputs to the atmosphere and could thus help to prevent dangerous climate change. However, the amount of olivine necessary for these applications is huge: It lies in the range of present-day global coal production (47). Compared to other techniques (8) olivine dissolution is very effective, rated as relatively safe, and moderately expensive. A huge dissolution peak of olivine in spatially restricted areas, e.g., near major mines, is limited by the saturation concentration of H_4SiO_4. It might have severe consequences for the alkalinity and *p*H of rivers (river alkalinization) or affect coastal zones. Thus ecosystem assessments for the expected impacts of the alkalinity rise are necessary before considering its implementation. If olivine is ground to very small grains of 10 μm, a complete dissolution within 1–2 y seems possible. Thus, the environmental impact in the regions of distribution might be minimized to the distribution itself without further side effects. However, a distribution in the densely vegetated interior of the tropical rain forest catchment area seems difficult to obtain. There remains the need to study in detail the impact of the proposed increase in alkalinity and silicic acid in soils and aquatic ecosystems.

Materials and Methods

For our carbon cycle simulations we use the carbon cycle box model BICYCLE, which was so far mainly used for paleo applications (48, 49). The model consists of ten oceanic reservoirs distinguishing surface, intermediate, and deep waters in three ocean basins (Atlantic, Southern Ocean, and Indo-Pacific), a well-mixed atmosphere, and a globally averaged scheme of the terrestrial biosphere containing seven boxes for C3 and C4 photosynthesis and soil carbon of three different turnover times. The carbonate system in the ocean has DIC and TA as state variables, from which all other variables (CO_2, partial pressure of CO_2, bicarbonate, carbonate, and *p*H) are calculated as functions of environmental conditions.

The anthropogenic emissions by fossil fuel combustion and land use change between A.D. 1750 and A.D. 2000 are taken from reconstructions (50, 51). From A.D. 2000 until A.D. 2100 we prescribe emissions following either the A2 or B1 emission scenarios of the IPCC (15). B1 emissions rise to a maximum of 12 Pg of C per year in 2050 and decline toward 6 Pg of C per year in 2100, while those in A2 rise steadily to 30 Pg of C per year in the year 2100 (Fig. 3*A*).

Because of the known model-dependent uncertainty of the climate-carbon cycle feedback (43), we do not propose a realistic temporal evolution of atmospheric CO_2 with or without geoengineering through enhanced silicate weathering under both emission scenarios. Our goal is merely to obtain a rough estimate for the magnitude and potential of the olivine dissolution geoengineering concept. We therefore restrict simulations to setups with (*i*) constant terrestrial carbon pools and (*ii*) a crude realization of the CO_2 fertilization to estimate the C sink potential of the terrestrial biosphere. The direct temperature effect of rising CO_2 is in our model affecting only sea surface temperature and thus the chemistry of the marine carbon cycle (mainly via CO_2 solubility) but not ocean circulation and mixing or C storage on land. Runs with these two scenarios should bracket the projected variation of the C cycle for the near future. We estimate the rising temperature of the atmosphere and the surface ocean as a function of atmospheric CO_2 by using a linear interpolation and extrapolation of the transient climate sensitivity of 2 K for the doubling of CO_2 from its preindustrial values (52).

Geoengineering is restricted to two scenarios, in which for the years 2010–2100 either 1 or 5 Pg of C per year (W_1 and W_5, respectively) are sequestrated by enhanced silicate weathering via olivine. Weathered bicarbonate enters the world ocean in the two equatorial basins by 50% each. These scenarios are applied to both emission scenarios A2 and B1 with and without dynamical terrestrial C storage leading to eight weathering simulations plus four non-weathering control runs.

ACKNOWLEDGMENTS. Locations of some major dunite mines have been provided by R.D. Schuiling. We furthermore thank P. Friedlingstein for providing C⁴MIP results, N. Moosdorf for preparing Fig. 2, and J. Bijma for discussions. P.K. and D.A.W.-G. were funded by PACES, the research program of AWI. The work of J.H. was supported through the German Science Foundation [Deutsche Forschungsgemeinschaft project HA 4472/6-1 and the Cluster of Excellence "CliSAP" (EXC177), University of Hamburg].

1. Doney SC, Fabry VJ, Feely RA, Kleypas JA (2009) Ocean acidification: The other CO_2 problem. *Annu Rev Mar Sci* 1:169–192.
2. Lenton TM, et al. (2008) Tipping elements in the Earth's climate system. *Proc Natl Acad Sci USA* 105:1786–1793.
3. Allen MR, et al. (2009) Warming caused by cumulative carbon emissions towards the trillionth tonne. *Nature* 458:1163–1166.
4. Meinshausen M, et al. (2009) Greenhouse-gas emission targets for limiting global warming to 2 °C. *Nature* 458:1158–1162.
5. Smith JB, et al. (2009) Assessing dangerous climate change through an update of the Intergovernmental Panel on Climate Change (IPCC) reasons for concern. *Proc Natl Acad Sci USA* 106:4133–4137.
6. Solomon S, Plattner G-K, Knutti R, Friedlingstein P (2009) Irreversible climate change due to carbon dioxide emissions. *Proc Natl Acad Sci USA* 106:1704–1709.
7. Lenton TM, Vaughan NE (2009) The radiative forcing potential of different climate geoengineering options. *Atmos Chem Phys* 9:5539–5561.
8. *Geoengineering the Climate: Science, Governance and Uncertainty* (Royal Society, London) www.royalsoc.ac.uk.
9. Crutzen PJ (2006) Albedo enhancement by stratospheric sulfur injections: A contribution to resolve a policy dilemma? *Clim Change* 77:211–220.
10. Caldeira K, Wood L (2008) Global and Arctic climate engineering: numerical model studies. *Philos Trans R Soc London A* 366:4039–4056.
11. Lackner KS (2002) Carbonate chemistry for sequestering fossil carbon. *Annu Rev Energy Environ* 27:193–232.
12. Lackner KS (2003) A guide to CO_2 sequestration. *Science* 300:1677–1678.
13. Keith D, Ha-Duong M, Stolaroff J (2006) Climate strategy with CO_2 capture from the air. *Clim Change* 74:17–45.
14. Stephens J, Keith D (2008) Assessing geochemical carbon management. *Clim Change* 90:217–242.
15. Nakićenović N, Swart R, eds. (2000) *Special Report on Emissions Scenarios. A special report of Working Group III of the Intergovernmental Panel on Climate Change* (Cambridge Univ Press, Cambridge, UK).
16. Steinacher M, Joos F, Frölicher TL, Plattner G-K, Doney SC (2009) Imminent ocean acidification in the Arctic projected with the NCAR global coupled carbon cycle-climate model. *Biogeosciences* 6:515–533.
17. Silverman J, Lazar B, Cao L, Caldeira K, Erez J (2009) Coral reefs may start dissolving when atmospheric CO_2 doubles. *Geophys Res Lett* 36:L05606.
18. Schuiling RD, Krijgsman P (2006) Enhanced weathering: An effective and cheap tool to sequester CO_2. *Clim Change* 74:349–354.
19. Lenton TM, Britton C (2006) Enhanced carbonate and silicate weathering accelerates recovery from fossil fuel CO_2 perturbations. *Global Biogeochem Cycles* 20:GB3009.
20. Uchikawa J, Zeebe RE (2008) Influence of terrestrial weathering on ocean acidification and the next glacial inception. *Geophys Res Lett* 35:L23608.
21. Beaulieu E, et al. (2010) Impact of atmospheric CO_2 levels on continental silicate weathering. *Geochem Geophys Geosyst* 11:Q07007.
22. Hangx SJ, Spiers CJ (2009) Coastal spreading of olivine to control atmospheric CO_2 concentrations: A critical analysis of viability. *Int J Greenhouse Gas Control* 3:757–767.
23. Kheshgi HS (1995) Sequestering atmospheric carbon dioxide by increasing ocean alkalinity. *Energy* 20:915–922.
24. Harvey LDD (2008) Mitigating the atmospheric CO_2 increase and ocean acidification by adding limestone powder to upwelling regions. *J Geophys Res* 113:C04028.
25. Rau GH (2008) Electrochemical splitting of calcium carbonate to increase solution alkalinity: Implications for mitigation of carbon dioxide and ocean acidity. *Environ Sci Technol* 42:8935–8940.
26. Zeebe RE, Wolf-Gladrow DA (2001) *CO_2 in Seawater: Equilibrium, Kinetics, Isotopes*, Elsevier Oceanography Book Series (Elsevier, Amsterdam), 65.

27. Plummer L, Busenberg E (1982) The solubilities of calcite, aragonite and vaterite in CO_2-H_2O solutions between 0 and 90 °C, and an evaluation of the aqueous model for the system $CaCO_3$-CO_2-H_2O. *Geochim Cosmochim Acta* 46:1011–1040.
28. Cappellen PV, Qiu L (1997) Biogenic silica dissolution in sediments of the Southern Ocean I. Solubility. *Deep-Sea Res Part II* 44:1109–1128.
29. Laruelle GG, et al. (2009) Anthropogenic perturbations of the silicon cycle at the global scale: Key role of the land-ocean transition. *Global Biogeochem Cycles* 23:GB4031.
30. Amiotte-Suchet P, Probst J-L, Ludwig W (2003) Worldwide distribution of continental rock lithology: Implications for the atmospheric/soil CO_2 uptake by continental weathering and alkalinity river transport to the oceans. *Global Biogeochem Cycles* 17:1038.
31. Richey JE, Melack JM, Aufdenkampe AK, Ballester VM, Hess LL (2002) Outgassing from Amazonian rivers and wetlands as a large tropical source of atmospheric CO_2. *Nature* 416:617–620.
32. Cole JJ, Caraco NF (2001) Carbon in catchments: Connecting terrestrial carbon losses with aquatic metabolism. *Mar Freshwater Res* 52:101–110.
33. Marotta H, Duarte CM, Sobek S, Enrich-Prast A (2009) Large CO_2 disequilibria in tropical lakes. *Global Biogeochem Cycles* 23:GB4022.
34. Körtzinger A (2003) A significant CO_2 sink in the tropical Atlantic Ocean associated with the Amazon River plume. *Geophys Res Lett* 30:2287.
35. Chapman L (2007) Transport and climate change: A review. *J Transport Geography* 15:354–367.
36. Pereira HS, Korndörfer GH, Vidal AD, de Camargo MS (2004) Silicon sources for rice crop. *Sci Agric (Piracicaba, Braz)* 61:522–528.
37. Hartmann J, Kempe S (2008) What is the maximum potential for CO_2 sequestration by stimulated weathering on the global scale? *Naturwissenschaften* 95:1159–1164.
38. Hartmann J, Jansen N, Dürr HH, Kempe S, Köhler P (2009) High-resolution global CO_2-consumption by chemical weathering: What is the contribution of hotspots? *Glob Planet Change* 69:185–194.
39. Van Cappellen P, Dixit S, van Beusekom J (2002) Biogenic silica dissolution in the oceans: Reconciling experimental and field-based dissolution rates. *Global Biogeochem Cycles* 16:1075.
40. Dugdale RC, Wilkerson FP (1998) Silicate regulation of new production in the equatorial Pacific upwelling. *Nature* 391:270–273.
41. Nelson DM, Tréguer P, Brzezinski MA, Leynaert A, Quéguiner B (1995) Production and dissolution of biogenic silica in the ocean: Revised global estimates, comparison with regional data and relationship to biogenic sedimentation. *Global Biogeochem Cycles* 9:359–372.
42. Bernard CY, Dürr HH, Heinze C, Segschneider J, Maier-Reimer E (2009) Contribution of riverine nutrients to the silicon biogeochemistry of the global ocean—a model study. *Biogeosciences Discussions* 6:1091–1119.
43. Friedlingstein P, et al. (2006) Climate-carbon cycle feedback analysis: Results from the C^4MIP model intercomparison. *J Climate* 19:3337–3353.
44. Zaehle S, Friedlingstein P, Friend AD (2010) Terrestrial nitrogen feedbacks may accelerate future climate change. *Geophys Res Lett* 37:L01401.
45. Etheridge DM, et al. (1996) Natural and anthropogenic changes in atmospheric CO_2 over the last 1000 years from air in Antarctic ice and firn. *J Geophys Res* 101(D2): 4115–4128.
46. Keeling RF, Piper S, Bollenbacher A, Walker J (2009) Atmospheric CO_2 records from sites in the SIO air sampling network. *Trends: A Compendium of Data on Global Change* (Carbon Dioxide Information Analysis Center, Oak Ridge Natl Laboratory, U.S. Department of Energy, Oak Ridge, TN).
47. *World Energy Outlook* (International Energy Agency, Paris) www.iea.org.
48. Köhler P, Fischer H, Munhoven G, Zeebe RE (2005) Quantitative interpretation of atmospheric carbon records over the last glacial termination. *Global Biogeochem Cycles* 19:GB4020.
49. Köhler P, Bintanja R (2008) The carbon cycle during the Mid Pleistocene Transition: The Southern Ocean decoupling hypothesis. *Climate of the Past* 4:311–332.
50. Houghton RA (2003) Revised estimates of the annual net flux of carbon to the atmosphere from changes in land use and land management 1850–2000. *Tellus B* 55:378–390.
51. Marland G, Boden T, Andres RJ (2005) Global, regional, and national CO_2 emissions. *Trends: A Compendium of Data on Global Change* (Carbon Dioxide Information Analysis Center, Oak Ridge Natl Laboratory, U.S. Department of Energy, Oak Ridge, TN).
52. Dufresne J-L, Bony S (2008) An assessment of the primary sources of spread of global warming estimates from coupled atmosphere-ocean models. *J Climate* 21:5135–5144.
53. Meybeck M, Dürr HH, Vörösmarty CJ (2006) Global coastal segmentation and its river catchment contributors: A new look at land-ocean linkages. *Global Biogeochem Cycles* 20:GB1S90.
54. Probst J, Mortatti J, Tardy Y (1994) Carbon river fluxes and weathering CO_2 consumption in the Congo and Amazon river basins. *Appl Geochem* 9:1–13.